Journal of Manufacturing Engineering, September 2018, Vol. 13, Issue.3, pp 158-164

REVIEW AND EXPERIMENTAL ON COMBINATION OF FE-PCL3 NANOPARTICLES BY MACHNOCHEMICAL DISPENSATION WITH BALL MILLING

***Srivijai B[1], Jegan A[2], Iniyaraja B[3] and Babu M[4]**

[1&3] Assistant Professor, Department of Mechanical Engineering, Mahendra Institute of Engineering &Technology, Namakkal, Tamil Nadu, India.

[2&4] Associated Professor, Department of Mechanical Engineering, Sona college of Technology , Salem, Tamil Nadu, India.

ABSTRACT

This paper reveals information on research of PCl_3 nanoparticles by milling using a planetary ball mill, taking the mixture of two different sizes of balls. The milled powder is characterized using X-ray diffraction (XRD) and particles size analyzer. Samples have taken at 0, 18, 24, 30 and 40 hours after milling the powder. The crystal sizes of milled powder for different milling times are characterized. By increasing the milling time crystal size decreases. After 40 hours average crystal size of milled powder is 21nm. But controlling the size and preparation in bulk of nanoparticles eco-friendly is interesting. This paper reports on preparation of PCl_3 nanoparticles by wet milling using a planetary ball mill, taking the combination of two different sizes of balls. The milled powder is characterized using X-ray diffraction (XRD) and particles size analyzer. Samples have taken at 18, 24, 36 and 50 hours after milling the powder. The crystal sizes of milled powder for different milling times are characterized. By increasing the milling time crystal size decreases. After 50 hours average crystal size of milled powder is 15nm.

There are a lot of parameters used in ball milling process. However, the parameters that have been tested most for optimization are the rotation speed and milling time. This indicates that these two parameters play an important role in determining the effectiveness of the milling. As supported by Samos, ball to powder weight ratio is recognized as one of the most influential parameters, alongside milling time and rotation speed. Zhang et al. believed that the volume of milling medium is the most influential parameter, followed by the rotation speed. The ball to powder weight ratio used by previous works clearly varies from one another. Although majority of the ratios used were in the range of 10: 1 to 20: 1, there are works that have used ratio much higher than that, going up to 100: 1 [4]. Higher ball to powder Weight ratio helps increase the particle size reduction rate. However, when the ratio used is too high, there is a possibility that contamination resulting from the collision of grinding balls and inner wall of milling vial will happen

Keywords: *Phosphorus Trichloride, Copper Nanoparticles, Ball Milling, Combination of Balls Milling.*

1. Introduction

Mechnochemical process makes use of improvement of chemical reactions by mechanical force. Ping and work fellow has synthesized a number of golden and chemical compound nanoparticles, such as Fe, Cu,PCl_3 Co, Ni, $Fe2O_3$, $Cr2O_3$, and $Al2O_3$, by machnochemical process employing a ball mill. in the present excrement, this proposal has been proposed to synthesize nano particles of non-equilibrium Fe- PCl_3 primary solid solution by the coincidental growth.

The Fe-Cu twin system possesses a large positive enthalpy of addition and so is sort of unmixable within the whole selection of work in balance. A solution of the Fe-Cl_3 system may be obtained solely by non-equilibrium techniques, such as mechanical alloying or vapour deposition. The reactions end in the formation of Fe- PCl_3 nanoparticles embedded within the matrix of by-product NaCl. Give that the degree fraction of $NaCl_3$ is satisfactorily giant, the metal nanoparticles separately nucleate and rise within the $NaCl_3$ atmosphere in this study, the quantity fraction of NaCl within the product mixture is planned to be 96.2%. Ensuing deletion of the

**Corresponding Author - E- mail: bsrivijai@gmail.com*

NaCl leads to the powder consisting of metric linear unit sized particles. NaCl powder additionally as another necessary role to contain combustive reaction throughout the edge [1-3].

In the previous investigation metallic element and PCl_3 nanoparticles were synthesize through the reactions and severally, and these reactions proceed with unstable grow itself combustion attributable to the big heat content changes within the reactions. The combustible reaction is undesirable for the synthesis of nanoparticles since it causes a big temperature rise, leading to an oversized particle size. Therefore, the suppression of the combustible reaction is vital for the synthesis of uniform sized nanoparticles during this method. The previous studies speculate that the combustion reaction could be initiated by ball/powder collision events throughout edge. Reduction of collision energy and dilution of reactants ar thought of because the attainable means that for avoiding comburent reaction. During this study, the combustion reaction was suppressed by adding NaCl powder into the beginning mixture, to decrease the collision frequency between the reactants.

This paper describes the results of a study on the evolution of nanostructures and magnetic properties throughout the mechanochemical process of Fe PCl_3 and PCl_3 with atomic number 10 to make Fe- PCl3 nanoparticles. it absolutely was conjointly found that the formation of thin polygon plates of Fe(OH)2 accompanies the Fe-Cl nanoparticles formation [4-6].

2. Tentative method

2.1 Combination of nanoparticles

The staring resources utilized in this revise were anhydrous $FePCl_3$ powder was intercalary as agent to the initial combine so as to avoid carburant reaction. The chloride powders were dried before edge. The beginning mixture (5g) that consists of $FePCl_3$ + PCl_3 + 5Na + 7$NaPCl_3$ was loaded and sealed beside Ø5.8mm steel balls (apx.17 g) in a very hardened steel ampoule below atmosphere. The reactants were polished victimization SPEX 8000 mixer/mill for numerous times (up to 80h). The container temperature was reserved stable in air cooling. The surface temperature of the bottle was monitor through the trail of edge by a Chromel-Alumel thermometer showing emotion concerned to its exterior. A sudden boost of the bottle temperature indicates that the carburant response occur. During this study, all the edge method was passed out exclusive of the comburent reaction. The Fe- PCl_3 nanoparticles were separated from NaCl through a following scour method. The as-milled powders were diffuse ultrasonically within the deionized and deoxy-genated water. Then, the Fe- PCl_3 particles and NaCl resolution were separated employing a magnet or a centrifuge. Once scour, the Fe- PCl3 particle was desiccated below vacuum at atmosphere temperature and overtly moves to a glove box set with air [7-9].

2.2 Description model of Nanoparticles

Composition examination of the scour powders was accepted out on a Siemens 5000 X-ray diffract meter with Ni-filtered PCl3-K_α emission may be generate at 40k/35mA. A scaled and Air stuffed example storage place was accustomed forestall oxidization of the instance. The analysis was applied on a sampling space of 200µmx160µm. Morphologies of the washed powders were experimental on a JEOL 6300F field production SEM (FESEM).

Morphologies, nanostructures and composition of the scour powders were investigated on Transmission Electron microscopy (TEM) employing a Phillips 430 equipped with a Gatan Imaging Filter GIF200 integrated in power loss prism spectroscope (EELS) for elementary mapping at an quickening voltage of 300Kv for potential unit. A sample controller within which taste-tester may well be preserved was used, so the sample was came upon within the TEM exclusive of expose to air. The synthesized nanoparticles were place onto a carbon layer supported on a copper grating straight from the scour powder, then the grating was loaded to the sampler innovate the glove box.

These appraisals were conjointly done on a high-resolution TEM (HRTEM) employing a JEOL JEM-2014 equipped with a NORAN traveler III EDX at quickening voltage of 200 kilovolt. Nanobeam optical phenomenon (NBD) mode on the JEM-2014 was accustomed gain lepton optical phenomenon patterns from entity nanoparticles. The synthesized nanoparticles were diffuse ultrasonically in iso-propylalcohol, and a couple of drops of the mixture were then pipetted onto a Ni grid simply before insertion into the JEM-2014 TEM, therefore minimizing the choice of corrosion in air.

Detailed exterior areas of the scour powders were calculated with the apx it have 5-point BET (Brunauer-Emmett-Teller) methodology employing a Micromeritics Gemini 2360. Mean diameters of particles were approximate from the precise expanse. Engaging power of the as-milled powders were distributed on AN Oxford 3001 moving example meter (VSM) with a most sensible ground of 2.4 MA/m in that region of temperature. The milled powders were cold pressed to the form of cylinder (Ø4.5mm × t3.5mm) in a glove box.

The pressed example were conserved and fixed in a polymer vial of 2.4 MA/m was taken to be the diffusion magnetization [10-17].

3. Grades and Conversation

Composition of the reveals excrement scour powder for a variety of milling times, analyze using the EDX in the SEM. The average work of the powders composed by using a magnet was around Fe-50 at %PCl3, somewhat lacking in PCl_3 than the nominal work (Fe-50.0 at %PCl3). On the other hand, the normal work of the powders composed by a centrifuge was roughly Fe-49.8 at %PCl3, easy to the study and work. It is due to that the synthesize PCl_3-rich particles could not be composed totally by using a magnet, as Fe clusters in the fcc-PCl_3 matrix perform as γ-Fe in which the magnetic instant of Fe atoms is very small. The powders collected using a centrifuge were bare to air in the course of collect, leading to the corrosion of Fe-PCl_3 nanoparticles.

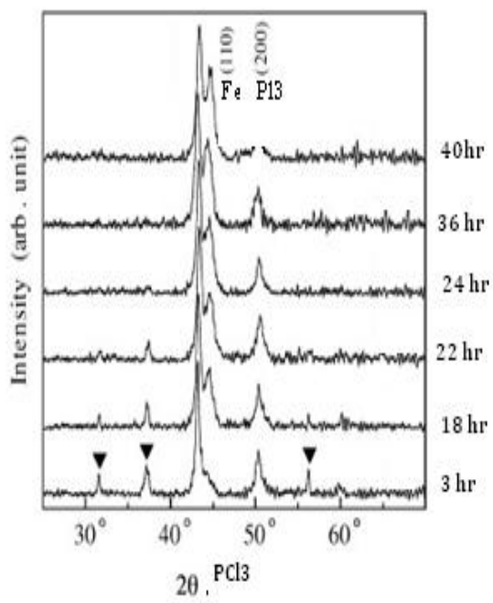

Figure 1 X-ray diffraction (XRD) patterns arrange of milling times.

Reveals the X-ray diffraction (XRD) patterns of the scour powders for arrange of milling times in Fig. 1. The edge corresponding to BCC and FCC phases could be recognized to provide that the pattern parameters of BCC and FCC phases were close to those of α-Fe and PCl_3, in that order. It can be seen that Fe and PCl3 particles are obtained after removing the left over reactants and NaCl by the suitable scour process. In the XRD pattern, the peaks other than those of Fe and PCl_3, denoted by the triangles in are found for the powders milled for shorter time apx<24h. Those tip position were closed to those of Fe $(OH)_2$.

The crystallite sizes of the scour Fe-PCl_3 nanoparticles were approximate using the Scherrer equation from the width of the PCl3 (200) tip in the XRD patterns.) Reveals the crystallite sizes of the washed nanoparticles for various milling times. The correction of the machine error was carried out with the Warren`s method, using PCl_3 powder with the purity of 99.998% and the particle size of 152 μm as the standard sample approximately. The crystallite size of PCl_3 has approximately 14 nm, and remained constant with milling time. The crystalline mass has as well estimated by TEM observations.

In the TEM images Fig. 2 intense field (BF) (b) and (e), and dim field (BF), (a), (c) and (d) of the scour Fe-PCl_3 nanoparticles after 50h, 50h, and 80h milling. In the DF images, the strongly reflecting regions corresponded to the rings of α-Fe (110) or PCl_3 (111). The DF images show that there is no remarkable difference in the crystalline size of Fe and Cl, and therefore it is suggested that both sizes are just about 15 nm with the Cu crystallite size estimated from the XRD tip in widths. The crystalline size remained constant with milling time, which was in good concurrence with the crystallite size [18-22].

Reveals the mean particle size estimated from the specific surface areas of the scour powders for various milling times in Fig. 3. The atom size increased with milling time, to be approximately 10nm and 50nm for powders milled for 3h and 80h, in that order. These results were also in good accord with those estimated from the TEM BF images shown in figure. Nevertheless, the particle size remains in the order of ten nanometers. It is inferred from these results that the near creation of NaCl productively suppressed the welding between particles throughout milling.

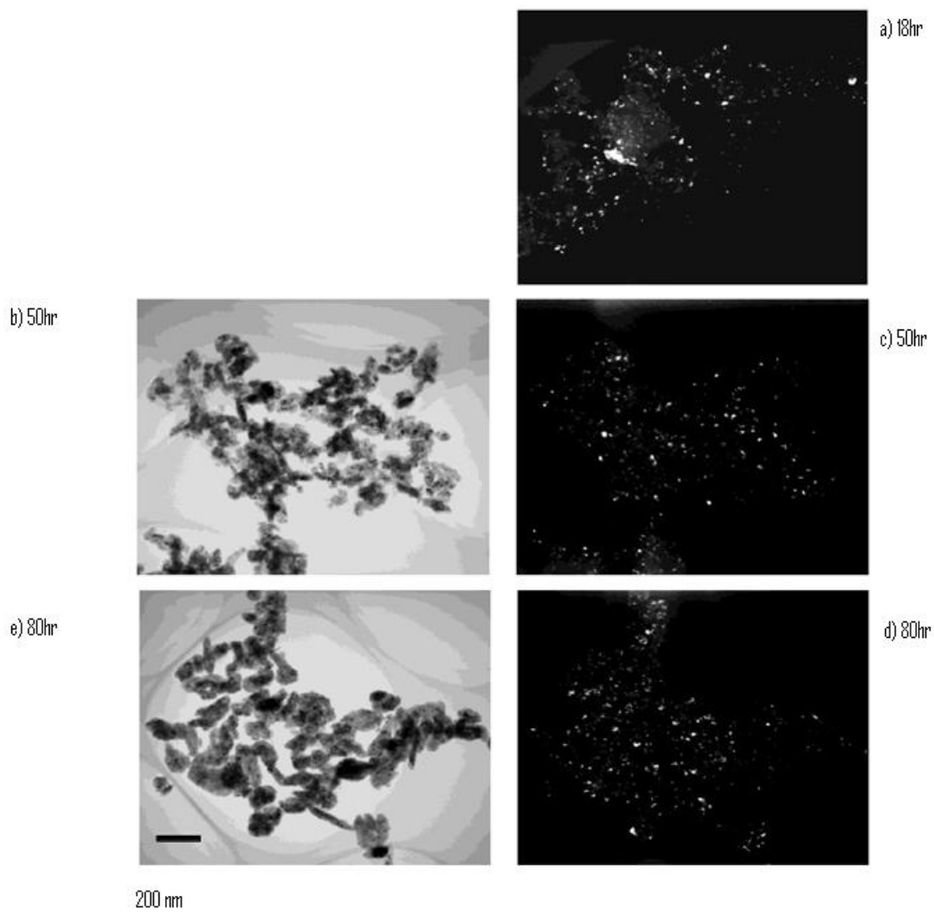

Figure 2 TEM images taken in intense field (BF) (b) and (e), and dim field (BF), (a), (c) and (d) of the scour Fe-PCl_3 nanoparticles after 50h, 50h, and 80h milling

Reveals the mean particle size estimated from the specific surface areas of the scour powders for various milling times in Fig. 3. The atom size increased with milling time, to be approximately 10nm and 50nm for powders milled for 3h and 80h, in that order. These results were also in good accord with those estimated from the TEM BF images shown in figure. Nevertheless, the particle size remains in the order of ten nanometers. It is inferred from these results that the near creation of NaCl productively suppressed the welding between particles throughout milling [23-25].

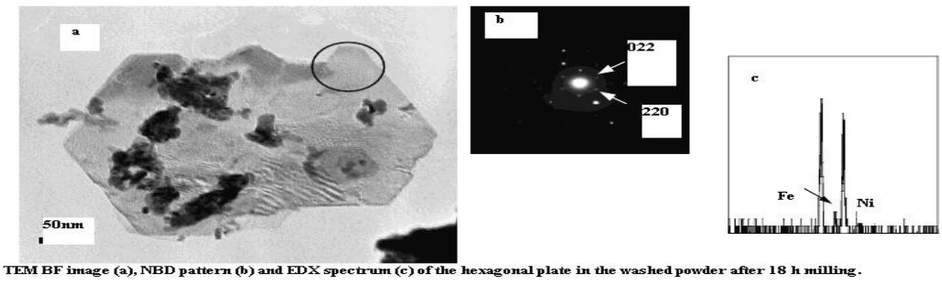

TEM BF image (a), NBD pattern (b) and EDX spectrum (c) of the hexagonal plate in the washed powder after 18 h milling.

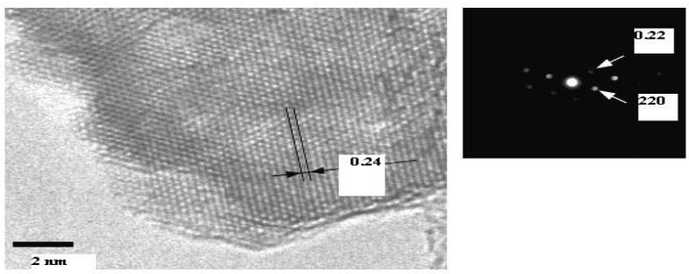

Figure 3 Shows the mapping images of milling carried out for 50 h reveals both Fe and Cl in the entire area of the particles, suggestive of that nanoparticles are a solid solution of the Fe-Cl system.

.

In the scour powder for 20h milling two kinds of morphologies were experiential, an uneven and a hexagonal form denoted by the pointer. The FESEM images also demonstrate such morphologies. The scour powder for 20 h milling incorporated the frequent hexagonal plates in comparison with the powder for 50h milling. The plates are usually with a width of a few nanometers and a diameter of around 300nm in the powder milled for 18h.

Even though the mean particle size improved linearly with milling time, the size movement away reach a maximum roughly 20 h milling. It is accredited to that the scour powder milled for roughly 20 h built-in the numerous hexagonal plates [26-31].

The TEM BF and necessary mapping images of Fe and PCl3 was using the imaging fresh for the scour powder after 50 h milling in Fig. 3. In the mapping images, the show from both Fe and Cl can be seen in the entire area of the particles, suggestive of that nanoparticles are a solid solution of the Fe-Cl system. The mapping images also display mottled contrasts due to the non-uniformity in the work. The size of the variation is lesser than the crystallite size (about 15 nm) determined by XRD pattern and the grain size determined by TEM DF image. Also the mapping images shows that the hexagonal plate does not contain Cl atoms because the sign from Cl_3 can scarcely be seen.

The arrangement and work of the hexagonal plate in the scour powder milled for 80h were exanimate by the HRTEM with the EDX, as are show in Fig.3. The NBD pattern and the EDX spectrum from the region covered with a circle in the TEM BF images are shown in 3 (b) and (c), respectively. The NBD pattern suggests that the hexagonal plates are α-Fe2O3 with [001] normal, and the EDX spectrum exhibited simply Fe peaks (Ni peaks were confirmed to be from a Ni grid). Also shows the HRTEM image and the NBD pattern of the hexagonal plate in the scour powder milled for 80h.

The lattice space was 0.24 nm, which was secure to the mention assessment of α-Fe2O3 {200} plane (0.25178nm18). It is consequently optional that the hexagonal plate is α-FeO with [001] normal. Though, the XRD patterns indicate that the hexagonal plates are Fe (OH)2. These grades optional that Fe (OH)2 was

changed into α-Fe2O3 by isopropyl alcohol that was used to go away the synthesized nanoparticles in the TEM explanation.

The method for the configuration of the hexagonal plates has not been clarified yet. In the earlier study of Fe nanoparticles synthesis with the reaction (1), Though, these hexagonal plates were not found,1-3) suggestive of that the survival of Cl catalyzed the structure of the plates. Also, Fe $(OH)_2$ plates give the impression to form in the course of scour because $Fe(OH)_2$ contains two hydroxyl radicals. The plates may be synthesized as a consequence of the enduring reactants and Fe-Cu_3 nanoparticles. Reveals the diffusion magnetization (Ms) and coercively (Hc) values of the as-milled powders for various milling time.

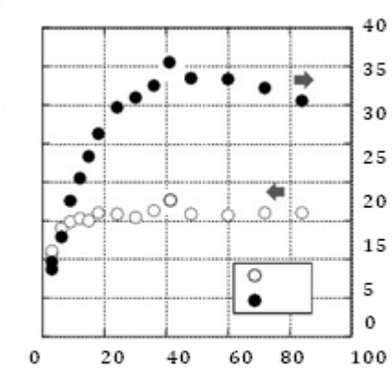

Figure 4 A graphical plot between milling time and particle size.

The Ms Standards increase quickly with milling time in the first 20 h milling, and level off upon further (> 20h) in the Fig. 4. The maximum Ms Values was around 14.9 μWb.m/kg, which was less important than the calculated Ms of 20.01 μWb.m/kg for the mixture Fe+PCl3+12NaCl. It is for the basis that the Fe cluster in the fcc- PCl_3 matrix acts as α-Fe phase) in which the magnetic flash of Fe atoms is extremely small. The growth of the response (1) during milling was incidental to nearly total after 20h milling from the change of the Ms value, for the reason that the bcc-Fe phase is ferromagnetic with a Ms of 270 μWb.m/kg at atmospheric temperature while the magnetizations of FePCl3, Na and PCl_3 are negligibly little. In count, the result of the work analysis indicates that the reactions (1) and (2) progress concurrently, for the reason that the composition of the synthesized Fe-PCl_3 nanoparticles for various milling times was forever closed to the supposed work (Fe-50.0 at %PCl_3). The H_c value greater than before with milling cause the decrease of the H values. The maximum H value was about 34.5 kA/m. This worth is a lot higher than that of the bulk α-Fe (about 0.1 kA/m). It is endorsed to that the particle size is closed to the critical size for a single magnetic area atom of Fe, which is 20-40nm) [31-35].

4. Conclusion

Fe-PCl_3 nanoparticles compressed by a mechanochemical exemption by a ball mill and a subsequent scour procedure were established to be a solid promise of the Fe-PCl_3 system. The element size was regular and around 50 nm after 80 h milling. The crystallite variety remained constant at something like 15 nm.

References

1. *Khayati G R and Jangharban K (2012), "The nanostructure Evolution of Ag powder synthesis by high energy ball milling", Advanced Powder Technology, Vol. 23, 393-397.*

2. *Satya V Ravikumar, Jay M Jha, Krishnayan Haldar, Surjya K Pal and Sudipto Chakraborty (2015), "Surfactant-Based Cu– Water Nanofluid Spray for Heat Transfer Enhancement of High Temperature Steel Surface" J. Heat Transfer, Vol. 137(5)102-110.*

3. *Ahmad Monshi, Mohammad Reza Foroughi and Mohammad Reza Monshi (2012), "Modified Scherrer Equation to Estimate More Accurately Nano-Crystallite Size Using XRD", World Journal of Nano Science and Engineering, Vol. 2, 154-160.*

4. *Khayati G R and Jangharban K (2012), "The nanostructure Evolution of Ag powder synthesis by high energy ball milling", Advanced Powder Technology, Vol. 23, 393-397.*

5. *Satya V Ravikumar, Jay M Jha, Krishnayan Haldar, Surjya K Pal and Sudipto Chakraborty (2015), "Surfactant-Based Cu–Water Nanofluid Spray for Heat Transfer Enhancement of High Temperature Steel Surface" J. Heat Transfer, Vol. 137 (5).*

6. *Ahmad Monshi, Mohammad Reza Foroughi and Mohammad Reza Monshi (2012), "Modified Scherrer Equation to Estimate More Accurately Nano-Crystallite Size Using XRD", World Journal of Nano Science and Engineering, Vol. 2, 154-160.*

7. *Jeong W J, Kim S K and Park G C (2006), "Preparation and characteristic of ZnO thin film with high and low resistivity for an application of solar cell", Thin Solid Films, Vol. 506-507, 180–183*

8. *Moritz M and Geszke-Moritz M (2013), "The newest achievements in synthesis, immobilization and practical applications of antibacterial nanoparticles", Chemical Engineering Journal, Vol. 228, 596–613.*

9. *Rekha K, Nirmala M, Nair M G, and Anukaliani A (2010), "Structural, optical, photocatalytic and antibacterial activity of zinc oxide and manganese doped zinc oxide*

nanoparticles," Physica B: Condensed Matter, Vol. 405 (15), 3180–3185.

10. *Nair S, Sasidharan A and Divya Rani V V (2009), "Role of size scale of ZnO nanoparticles and microparticles on toxicity toward bacteria and osteoblast cancer cells", Journal of Materials Science: Materials in Medicine, Vol. 20 (1), S235–S241.*

11. *Reinert A A, Payne C, Wang L, Ciston J, Zhu Y and Khalifah P G (2013), "Synthesis and characterization of visible light absorbing (GaN) 1-x(ZnO)x semiconductor nanorods", Inorganic Chemistry, Vol. 52 (15) 8389–8398.*

12. *Ludi B and Niederberger M (2013), "Zinc oxide nanoparticles: chemical mechanisms and classical and non-classical crystallization", Dalton Transactions, Vol. 42 (35), 12554–12568.*

13. *Vanmaekelbergh C and Van Vugt L K (2011), "ZnO nanowire lasers", Nanoscale, Vol. 3 (7), 2783–2800.*

14. *Wang Z L (2004), "Zinc oxide nanostructures: growth, properties and applications", Journal of Physics Condensed Matter, Vol. 16 (25), R829–R858.*

15. *Osmond M J and McCall M J (2010), "Zinc oxide nanoparticles in modern sunscreens: an analysis of potential exposure and hazard", Nanotoxicology, Vol. 4 (1), 15–41.*

16. *Darvin M E, König K and Kellner-Hoeferetal M (2012), "Safety assessment by multiphoton fluorescence/second harmonic generation/hyper-Rayleigh scattering tomography of ZnO nanoparticles used in cosmetic products", Skin Pharmacology and Physiology, Vol. 25 (4), 219–226.*

17. *Darvin M E, Haag S, Meinke M, Zastrow L, Sterry W, and Lademann J (2010), "Radical production by infrared A irradiation in human tissue", Skin Pharmacology and Physiology, Vol. 23 (1), 40–46.*

18. *Darvin M E, Haag S F, Lademann J, Zastrow L, Sterry W and Meinke M C (2010), "Formation of free radicals in human skin during irradiation with infrared light", Journal of Investigative Dermatology, Vol. 130 (2), 629–631.*

19. *Baroli B (2010), "Penetration of nanoparticles and nanomaterials in the skin: fiction or reality", Journal of Pharmaceutical Sciences, Vol. 99 (1), 21–50.*

20. *Zhou G F and Bakker H, "Atomically disordered nanocrystalline Co2Si by high-energy ball milling," Journal of Physics Condensed Matter, vol. 6, no. 22, pp. 4043–4052, 1994.*

21. *Lemine O M, Louly M A, and Al-Ahmari A.M (2010), "Planetary milling parameters optimization for the production of ZnO nanocrystalline," International Journal of Physical Sciences, Vol.5,(17), 2721–2729.*

22. *Nguyen T D and Do T O (2011), "Size- and Shape-Controlled Synthesis of Monodisperse Metal Oxide and Mixed Oxide Nanocrystalsed", In Tech Publishers, Canada, 55.*

23. *Suryanarayana, (2001), "Mechanical alloying and milling," Progress in Materials Science, vol. 46 (1-2),1–184.*

24. *Zhao W, Fang M, Wu F, Wu H, Wang L and Chen G (2010), "Preparation of graphene by exfoliation of graphite using wet ball milling", Journal of Materials Chemistry, Vol. 20 (28), 5817–5819.*

25. *Mahamat A, Rani A and Husain P (2012), "Behavior of Cu-WC-Ti metal composite after using planetary ball milling", International Journal of Engineering and Applied Sciences, 278–282.*

26. *Wang Y and Forssberg E (2006), "Production of carbonate and silica nano-particles in stirred bead milling," International Journal of Mineral Processing, Vol. 81 (1), 1–14.*

27. *Hubert M, Petracovschi E, Zhang X H and Calvez L (2013), "Synthesisof Germanium-Gallium-Tellurium (Ge-Ga-Te) ceramics by ball-milling and sintering," Journal of the American Ceramic Society, Vol. 96 (5), 1444–1449.*

28. *Alvarez P, Llamazares J L S and Perez M J (2008), "Microstructural and magnetic characterization of Nd2Fe17 ball milled alloys", Journal of Non-Crystalline Solids, Vol. 354 (47–51), 5172–5174.*

29. *Ahmeda T and Mamat O (2011), "Characterization and properties of copper-silica sand nanoparticle composites", Defect and Diffusion Forum, Vol. 319-320, 95–105.*

30. *Esme U (2009), "Application of Taguchi method for the optimization of resistance spot welding process", The Arabian Journal For Science and Engineering, Vol. 34 (2), 519–528.*

31. *Halim S C (2007), "Flame spray synthesis of nanoparticles for food applications: synthesis, characterization, potential hazards, cost and scalability", Proceedings of the AIChE Annual Meeting, Salt Lake City, Utah, USA.*

32. *Guoxian L, Erde W and Zhongren W (1995), "Effects of ball-milling intensity on the amorphization rate of mixedNi50Ti50 powders", Journal of Materials Processing Technology, Vol. 51 (1–4), 122–130.*

33. *Akcay K, Sirkecioglu A, Tatlıerb M, Savas¸O T and Erdem-S¸enatalar A (2004), "Wet ball milling of zeolite HY", Powder Technology, Vol. 142 (2-3), 121–128.*

34. *Hedayati M, Salehi M, Bagheri R, Panjepour M and Maghzian A (2011), "Ball milling preparation and characterization of poly (ether ether ketone)/surface modified silica nanocomposite", Powder Technology, Vol. 207 (1–3), 296–303.*

35. *Zhang D, Cai R, Zhou Y, Shao Z, Liao X Z and Ma Z F (2010), "Effect of milling method and time on the properties and electrochemical performance of LiFePO4/C composites prepared by ball milling and thermal treatment", Electrochimica Acta, Vol. 55 (8),2653–2661.*